Organometallic Oxides: Oxidation of the Cubane $[(\eta\text{-}C_5R_5)Cr(\mu_3\text{-}O)]_4$ and the Structures and Magnetic Properties of the Salts $\{[(\eta\text{-}C_5R_5)Cr(\mu_3\text{-}O)]_4\}\{tcnq\}$ and $\{[(\eta\text{-}C_5R_5)Cr(\mu_3\text{-}O)]_4\}\{BF_4\}$

Daryl P. Allen,[†] Frank Bottomley,*[,†] Robert W. Day,[†] Andreas Decken,[†] Victor Sanchez,[‡] David A. Summers,[‡] and Robert C. Thompson[‡]

Department of Chemistry, University of New Brunswick, P.O. Box 45222, Station A, Fredericton, New Brunswick, E3B 6E2, Canada, and Department of Chemistry, University of British Columbia, 2036 Main Mall, Vancouver, British Columbia, V6T 1Z1, Canada

Received December 14, 2000

Differential pulse and current voltammetry for the cubane-like clusters $[(\eta\text{-}C_5R_5)Cr(\mu_3\text{-}O)]_4$ (R = H, Me; $R_5 = H_4Me$) showed that $[(\eta\text{-}C_5H_4Me)Cr(\mu_3\text{-}O)]_4$ and $[(\eta\text{-}C_5Me_5)Cr(\mu_3\text{-}O)]_4$ were oxidized to $\{[(\eta\text{-}C_5R_5)Cr(\mu_3\text{-}O)]_4\}^+$ and then to $\{[(\eta\text{-}C_5R_5)Cr(\mu_3\text{-}O)]_4\}^{2+}$, but $[(\eta\text{-}C_5H_5)Cr(\mu_3\text{-}O)]_4$ was oxidized only to $\{[(\eta\text{-}C_5H_5)Cr(\mu_3\text{-}O)]_4\}^+$. Oxidation of $[(\eta\text{-}C_5Me_5)Cr(\mu_3\text{-}O)]_4$ (**1**) by $AgBF_4$ or tcnq gave $\{[(\eta\text{-}C_5Me_5)Cr(\mu_3\text{-}O)]_4\}\{BF_4\}$ (**2**) or $\{[(\eta\text{-}C_5Me_5)Cr(\mu_3\text{-}O)]_4\}\{tcnq\}$ (**3**). It was shown by X-ray diffraction that the average Cr−Cr, Cr−O, and Cr−Cp* distances in **2** and **3** were 0.034(2), 0.007(5), and 0.02(1) Å shorter than those in **1**, respectively. Compounds **1**, **2**, and **3** were antiferromagnetic, with similar intracluster exchange coupling constants, J (−262(23), −211(34), and −266(46) cm^{-1}, respectively). There was coupling between unpaired electrons on $\{[(\eta\text{-}C_5Me_5)Cr(\mu_3\text{-}O)]_4\}^+$ and $\{tcnq\}^-$ in **3** at temperatures below 110 K.

Introduction

There have been a number of recent reports of single-molecule magnets.[1−3] The cores of these compounds are distorted cubane-like $[M(\mu_3\text{-}O)]_4$ units (M = Mn,[1] V,[2] Fe[3]). In an attempt to prepare compounds that exhibit exchange interactions leading to interesting magnetic properties, we are investigating compounds containing a tetrahedral $[(\eta\text{-}C_5R_5)M]_4$ unit (M = d-block metal), such as cubane-like clusters of general formula $[(\eta\text{-}C_5R_5)M(\mu_3\text{-}A)]_4$ (A = "hard" p-block element, O or N) and the adamantane-like clusters $[(\eta\text{-}C_5R_5)M]_4(\mu\text{-}A)_6$.[4−9] The cubanes $[(\eta\text{-}C_5Me_5)M(\mu_3\text{-}N)]_4$ (M = Ti,[10] V[6]) were diamagnetic, $[(\eta\text{-}C_5Me_5)V(\mu_3\text{-}O)]_4$ was paramagnetic (μ_{eff} = 2.35 μ_B at 300 K),[5] $[(\eta\text{-}C_5R_5)Cr(\mu_3\text{-}O)]_4$ (R = H,[9] Me[7] or $R_5 = H_4Me$)[11] were antiferromagnetic, and $[(\eta\text{-}C_5Me_5)M]_4(\mu\text{-}O)_6$ (M = Ti,[12] V[5]) were diamagnetic. It occurred to us that intermolecular exchange interactions might occur in salts of the type $\{cluster\}^+\{cluster\}^-$, where cluster = $[(\eta\text{-}C_5R_5)M(\mu_3\text{-}A)]_4$ or $[(\eta\text{-}C_5Me_5)M]_4(\mu\text{-}A)_6$. In this context, we describe here the electrochemistry of $[(\eta\text{-}C_5R_5)Cr(\mu_3\text{-}O)]_4$, the chemical oxidation of $[(\eta\text{-}C_5Me_5)Cr(\mu_3\text{-}O)]_4$ (**1**) by $AgBF_4$ or 7,7,8,8-tetracyanoquinodimethane (tcnq), and the solid-state structure and magnetic properties of $\{[(\eta\text{-}C_5Me_5)Cr(\mu_3\text{-}O)]_4\}\{BF_4\}$ (**2**) and $\{[(\eta\text{-}C_5Me_5)Cr(\mu_3\text{-}O)]_4\}\{tcnq\}$ (**3**).

Experimental Section

General Information. All manipulations were performed using a double-manifold vacuum/argon line. An undivided three-electrode glass cell that could be attached to the vacuum line was used for the electrochemical experiments. Solvents were predried, stored on the vacuum line over a drying agent, and distilled directly onto reagents or into the cell. The clusters $[(\eta\text{-}C_5R_5)Cr(\mu_3\text{-}O)]_4$ (R = H,[9,13] Me[7] or $R_5 = H_4Me$[9,11]) were prepared by the literature methods. Crystalline $LiAsF_6$ was purchased from Aldrich; adsorbed dioxygen was removed by crushing the crystals with a stir-bar under alternate vacuum and argon atmospheres.

Electrochemical experiments were conducted using a PAR 270-1 system. The working electrode was platinum foil (2 cm^2),

* Corresponding author. E-mail: bottomly@unb.ca.
[†] University of New Brunswick.
[‡] University of British Columbia.

(1) Aubin, S. M. J.; Sun, Z.; Pardi, L.; Krzystek, J.; Folting, K.; Brunel, L.-C.; Rheingold, A. L.; Christou, G.; Hendrickson, D. N. *Inorg. Chem.* **1999**, *38*, 5329.
(2) Castro, S. L.; Sun, Z.; Grant, M. G.; Bollinger, J. C.; Hendrickson, D. N.; Christou, G. *J. Am. Chem. Soc.* **1998**, *120*, 2365.
(3) Sangregorio, C.; Ohm, T.; Paulsen, C.; Sessoli, R.; Gatteschi, D. *Phys. Rev. Lett.* **1997**, *78*, 4645.
(4) Bottomley, F.; Sanchez, V.; Thompson, R. C.; Womiloju O. O.; Xu, Z. *Can. J. Chem.* **2000**, *78*, 383.
(5) Abernethy, C. D.; Bottomley, F.; Decken, A.; Summers, D. A.; Thompson, R. C. *Organometallics* **1999**, *18*, 870.
(6) Abernethy, C. D.; Bottomley, F.; Decken, A.; Cameron, T. S. *Organometallics* **1996**, *15*, 1758.
(7) Bottomley, F.; Chen, J.; MacIntosh, S. M.; Thompson, R. C. *Organometallics* **1991**, *10*, 906.
(8) Bottomley, F.; Magill, C. P.; Zhao, B. *Organometallics* **1990**, *9*, 1700.
(9) Bottomley, F.; Paez, D. E.; Sutin, L.; White, P. S.; Köhler, F.; Thompson, R. C.; Westwood, N. P. C. *Organometallics* **1990**, *9*, 2443.
(10) Gómez-Sal, P.; Martin, A.; Mena, M.; Yélamos, C. *J. Chem. Soc., Chem. Commun.* **1995**, 2185.
(11) Eremenko, I. L.; Nefedov, S. E.; Pasynskii, A. A.; Orazsakhatov, B.; Ellert, O. G.; Struchkov, Yu. T.; Yanovsky, A. I.; Zagorevsky, D. V. *J. Organomet. Chem.* **1989**, *368*, 185.
(12) Babcock, L. M.; Klemperer, W. G. *Inorg. Chem.* **1989**, *28*, 2003.
(13) Bottomley, F.; Paez, D. E.; White, P. S. *J. Am. Chem. Soc.* **1982**, *104*, 5651.

10.1021/om001067y CCC: $20.00
Publication on Web 03/31/2001

the counter electrode was a spiral of silver wire, the reference electrode was silver wire, and the electrolyte was $LiAsF_6$ in tetrahydrofuran (thf) as solvent. Using this cell and electrodes, the $E_{1/2}$ of the $(\eta\text{-}C_5H_5)_2Fe/(\eta\text{-}C_5H_5)_2Fe^+$ couple was measured as +0.097 V. All potentials are quoted with reference to $(\eta\text{-}C_5H_5)_2Fe/(\eta\text{-}C_5H_5)_2Fe^+$.

Magnetic susceptibilities were measured on a Quantum Design (MPMS) SQUID magnetometer at the Advanced Materials and Process Engineering Laboratory (AMPEL) at the University of British Columbia. Measurements were made over the temperature range 2−300 K at an applied field of 10 000 G, and susceptibilities were corrected for the background signal from the sample holder at all temperatures. The susceptibilities were corrected for the diamagnetism of all atoms using Pascal's constants,[14] and they are reported per mole of cluster. ^{1}H NMR spectra were measured on Varian XL200 or Unity 400 spectrometers. The mass spectra were measured by EI (70 eV) or by FAB (in a 3-nitrobenzyl alcohol matrix) methods on a Kratos MS 50 instrument. Infrared spectra were measured as KBr pellets or Nujol mulls on a Perkin-Elmer 683 instrument. EPR spectra of powdered samples of **2** and **3** were recorded on a modified version of a Varian E-4 spectrometer at room temperature and 9.170 GHz, at UNB. The field was referenced to α,α-diphenyl-β-picrylhydrazyl (dpph). The spectrum of **3** was also recorded on a Bruker ECS 106 spectrometer at room temperature and at 120 K and 9.8 GHz at UBC, where the field was referenced to peroxylamine disulfonate. Microanalyses were by Galbraith Laboratories, Knoxville, TN, and by the University of British Columbia microanalytical facility.

Preparation of $\{[(\eta\text{-}C_5Me_5)Cr(\mu_3\text{-}O)]_4\}\{BF_4\}$ (2). Unless noted, operations were conducted in the dark. To a solution of $[(\eta\text{-}C_5Me_5)Cr(\mu_3\text{-}O)]_4$ (0.30 g, 0.37 mmol) in tetrahydrofuran (250 cm^3) was added, with stirring, a solution of $AgBF_4$ (0.26 g, 1.33 mmol) in tetrahydrofuran (100 cm^3). The mixture was stirred for 16 h, giving a black suspension in a gray solution. The mixture was filtered through Celite, giving a colorless filtrate, which was discarded, and a purple-black residue, onto which CH_2Cl_2 (100 cm^3) was condensed. The resulting mixture was again filtered through Celite, giving a purple-gray residue that was discarded and a deep purple filtrate. The filtrate was concentrated to 50 cm^3 under vacuum and then ether (30 cm^3) condensed onto it, in the light. A deep purple precipitate of **2** formed on setting aside for 24 h at room temperature. This was collected by filtration and recrystallized from CH_2Cl_2. Yield: 0.158 g, 48%.

Characterization of 2. Anal. Found: C, 52.5, 52.2; H, 6.6, 6.6. Calcd for $C_{40}H_{60}BCr_4F_4O_4$: C, 53.4; H, 6.7. A low carbon analysis was also obtained for $\{[(\eta\text{-}C_5Me_5)Cr(\mu_3\text{-}O)]_4\}\{tcnq\}$ (see below) and for $[(\eta\text{-}C_5Me_5)Cr(\mu_3\text{-}O)]_4$: C, 57.9; H, 7.2. Calcd for $C_{40}H_{60}Cr_4O_4$: C, 59.1, H, 7.4. The reason for these low carbon analyses, which have been observed previously,[4,15,16] is not known. NMR: ^{1}H (C^2HCl_3 solution): −3.08 ppm ($\Delta\nu_{1/2}$ = 24.1 Hz). IR (Nujol mull): 1025 cm^{-1}, vs, ν(B−F). Mass spectrum (FAB) (*m/e*, % relative intensity, assignment): 812, 100, $\{[(C_5Me_5)CrO]_4\}^+$; 677, 42, $\{(C_5Me_5)_3Cr_4O_4\}^+$; 542, 7.9, $\{(C_5Me_5)_2Cr_4O_4\}^+$; 272, 19.7, $\{(C_5Me_5)Cr_4O_4\}^+$. The compound did not show an EPR resonance at room temperature. It was also characterized by X-ray diffraction (see below).

Preparation of $\{[(\eta\text{-}C_5Me_5)Cr(\mu_3\text{-}O)]_4\}\{tcnq\}$ (3). To a solution of $[(\eta\text{-}C_5Me_5)Cr(\mu_3\text{-}O)]_4$ (0.20 g, 0.25 mmol) in tetrahydrofuran (150 cm^3) was added a solution of tcnq (0.075 g, 0.37 mmol) in tetrahydrofuran (50 cm^3). The mixture was stirred for 16 h and then filtered, giving a deep green filtrate and a small quantity of a green-brown residue, which was discarded. The filtrate was concentrated to 75 cm^3 under vacuum and then set aside at 4 °C for 3 weeks. Dark green crystals, which were shown to be $\{[(\eta\text{-}C_5Me_5)Cr(\mu_3\text{-}O)]_4\}\{tcnq\}(thf)_{0.5}$ by X-ray diffraction, were obtained. Yield: 0.167 g, 64%.

Table 1. Crystal Data for $\{[(\eta\text{-}C_5Me_5)Cr(\mu_3\text{-}O)]_4\}\{BF_4\}$ (2) and $\{[(\eta\text{-}C_5Me_5)Cr(\mu_3\text{-}O)]_4\}\{tcnq\}(thf)_{0.5}$ (3(thf)$_{0.5}$)

	2	**3**(thf)$_{0.5}$
empirical formula	$C_{40}H_{60}BCr_4F_4O_4$	$C_{54}H_{68}Cr_4N_4O_{4.5}$
M_r	899.69	1053.12
temp (K)	296(1)	296(1)
wavelength (Å)	0.710 73	1.541 78
cryst syst	tetragonal	triclinic
space group	$I\bar{4}$	$P\bar{1}$
a (Å)	11.587(2)	11.179(3)
b (Å)	11.587(2)	12.252(2)
c (Å)	15.151(3)	20.061(6)
α (deg)	90	100.94(2)
β (deg)	90	90.90(2)
γ (deg)	90	104.88(2)
V (Å^3)	2034.2(4)	2601(1)
Z	2	2
D_{calcd} (g cm^{-3})	1.469	1.345
F(000)	938	1104
cryst size (mm)	0.10 × 0.10 × 0.22	0.35 × 0.20 × 0.003
radiation	Mo Kα	Cu Kα
abs coeff (mm^{-1})	1.097	7.086
abs corr	φ scans	φ scans
min. − max. transmn	0.92−1.00	0.44−1.00
θ range collected (deg)	2.69−30.04	3.81−63.56
no. of reflns collected	1683	8879
no. of ind reflns	1675	8435
R_{int}	0.054	0.085
no. of reflns in refinement	1675	8423
no. of params refined	127	645
GoF (F^2)	1.033	1.028
R_1[a] ($I > 2\sigma(I)$)	0.0447	0.0553
R_1 (all data)	0.1977	0.2437
wR_2[b] ($I > 2\sigma(I)$)	0.1021	0.1379
wR_2 (all data)	0.1446[3]	0.2270[4]
largest/mean Δ/σ	0.001/0.000	0.045/0.001
min./max. ΔF (e Å^{-3})	−0.796/0.421	−0.483/0.480

[a] $R_1 = \sum||F_o| - |F_c||/\sum|F_o|$. [b] $wR_2 = (\sum[w(F_o^2 - F_c^2)^2]/\sum[wF_o^4])^{1/2}$. [c] weight = $1/[\sigma^2(F_o^2) + (0.055P)^2]$, where $P = ((F_o^2)_{max} + 2F_c^2)/3$. [d] weight = $1/[\sigma^2(F_o^2) + (0.08P)^2 + 4.00P]$, where $P = ((F_o^2)_{max} + 2F_c^2)/3$.

Characterization of 3. Anal. Found: C, 60.7; H, 6.0; N, 5.3. Calcd for $C_{54}H_{68}Cr_4N_4O_{4.5}$ ($\{[(C_5Me_5)CrO]_4\}\{tcnq\}0.5(thf)$): C, 61.6; H, 6.5; N, 5.3. Calcd for $C_{52}H_{64}Cr_4N_4O_4$ ($\{[(C_5Me_5)CrO]_4\}\{tcnq\}$): C, 61.4; H, 6.35; N, 5.5. The low carbon analysis is discussed above. NMR: ^{1}H (C^2HCl_3 solution): −3.16 ppm ($\Delta\nu_{1/2}$ = 34.8 Hz). IR (Nujol mull): 2175, 2150 cm^{-1}, w, ν(C−N). EPR (tetrahydrofuran solution): multiplet centered at g = 2.002, assigned to $\{tcnq\}^-$.

X-ray Diffraction. Crystals of **2** were obtained on setting aside a saturated CH_2Cl_2 solution for one month at room temperature. Crystals of **3**, as the tetrahydrofuran adduct, were obtained from tetrahydrofuran, as described above. Both compounds were harvested by scooping them into air-free Apiezon grease. Crystals suitable for X-ray diffraction were mounted, under argon, in capillaries, which were then sealed under vacuum. Diffraction data were obtained on a Rigaku AFC5R diffractometer, equipped with a rotating anode, at Dalhousie University. Details of the crystals, data collection, and data refinement are given in Table 1. The data were processed using the Siemens SHELXTL system, release 4.21. Hydrogen atoms were included in calculated positions and riding on the appropriate atom, with a general isotropic U. Refinement was by full-matrix least-squares on F^2. Labeled thermal ellipsoid plots of the $\{[(\eta\text{-}C_5Me_5)Cr(\mu_3\text{-}O)]_4\}$ units in **2** and **3** are shown in Figures 1 and 2, respectively; the tcnq

(14) König, E. In *Landolt-Börnstein, New Series, Vol. II/2*; Hellwege, K. H., Hellwege, A. M., Eds.; Springer-Verlag: Berlin, 1966.
(15) Fettinger, J. C.; Keogh, D. W.; Poli, R. *J. Am. Chem. Soc.* **1996**, *118*, 3617.
(16) Jandciu, E. W.; Kuzelka, J.; Legzdins, P.; Rettig, S. J.; Smith, K. M. *Organometallics* **1999**, *18*, 1994.

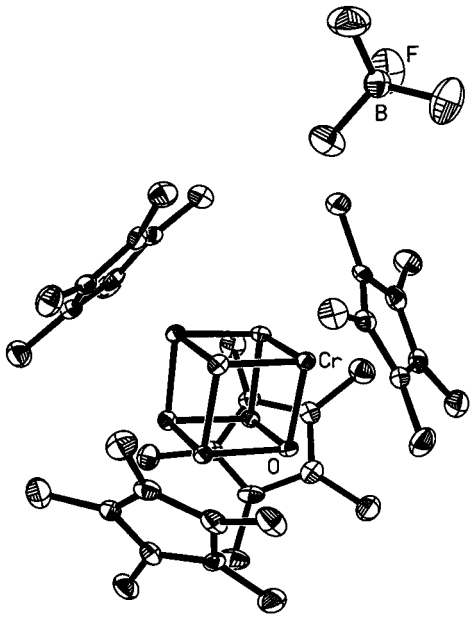

Figure 1. Thermal ellipsoid plot (30% probability) of $\{[(\eta\text{-}C_5Me_5)Cr(\mu_3\text{-}O)]_4\}\{BF_4\}$ (**2**).

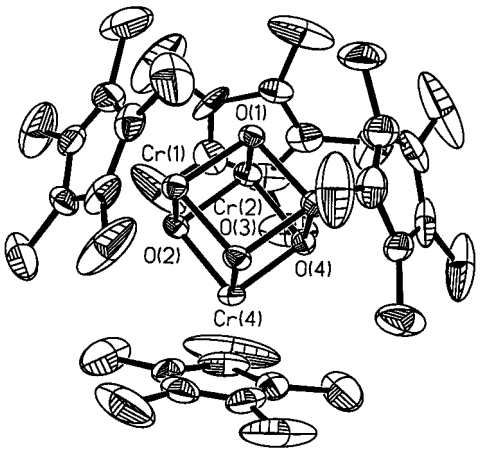

Figure 2. Thermal ellipsoid plot (30% probability) of the $\{[(\eta\text{-}C_5Me_5)Cr(\mu_3\text{-}O)]_4\}$ unit of **3**.

Table 2. Distances and Angles in $\{[(\eta\text{-}C_5Me_5)Cr(\mu_3\text{-}O)]_4\}\{BF_4\}$ (2)

distance (Å)		angle (deg)	
Cr−Cr(1)	2.781(2)	Cr−O−Cr(1)	91.9(2)
Cr−Cr(2)	2.815(2)	Cr−O−Cr(2)	93.3(2)
Cr−Cr(3)	2.815(2)	Cr−O−Cr(3)	92.8(2)
Cr−O	1.941(5)	O−Cr−O(1)	87.9(2)
Cr−O(1)	1.927(5)	O−Cr−O(2)	86.7(2)
Cr−O(2)	1.945(5)	O−Cr−O(3)	87.1(2)
Cr−Cp*[a]	1.909(8)	F−B−F(4)	110.5(3)
B−F	1.375(6)	F−B−F(5)	110.5(3)
		F−B−F(6)	107.4(6)

[a] Cp* is the centroid of the C_5 ring of the $(\eta\text{-}C_5Me_5)$ ligand.

unit of **3** is shown in Figure 3. Important distances and angles in the $\{[(\eta\text{-}C_5Me_5)Cr(\mu_3\text{-}O)]_4\}$ units of **2** and **3** and in the tcnq unit of **3** are given in Tables 2, 3, and 4, respectively. Full details are available in the Supporting Information.

Results and Discussion

Electrochemistry of $[(\eta\text{-}C_5R_5)Cr(\mu_3\text{-}O)]_4$. The electrochemistry of $[(\eta\text{-}C_5R_5)Cr(\mu_3\text{-}O)]_4$ was explored using cyclic voltammetry, differential pulse voltammetry, and

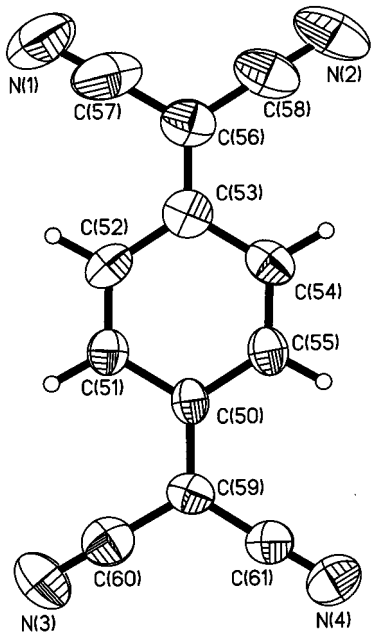

Figure 3. Thermal ellipsoid plot (30% probability) of the tcnq unit of **3**. The distances C(51)−C(52) and C(54)−C(55) are distance a in the Kistenmacher relationship,[20] C(50)−C(51), C(50)−C(55), C(52)−C(53), and C(53)−C(54) are distance b, C(50)−C(59) and C(53)−C(56) are distance c, and C(56)−C(57), C(56)−C(58), C(59)−C(60), and C(59)−C(61) are distance d.

Table 3. Distances and Angles in the $\{[(\eta\text{-}C_5Me_5)Cr(\mu_3\text{-}O)]_4\}$ Unit of 3

distance (Å)		angle (deg)	
Cr(1)−Cr(2)	2.831(2)	O(3)−Cr(1)−O(2)	87.9(2)
Cr(1)−Cr(3)	2.774(2)	O(3)−Cr(1)−O(1)	88.2(2)
Cr(1)−Cr(4)	2.781(2)	O(2)−Cr(1)−O(1)	87.0(2)
Cr(2)−Cr(3)	2.798(2)	O(1)−Cr(2)−O(4)	87.0(2)
Cr(2)−Cr(4)	2.818(2)	O(1)−Cr(2)−O(2)	86.3(2)
Cr(3)−Cr(4)	2.774(2)	O(2)−Cr(2)−O(4)	86.6(2)
Cr(1)−O(1)	1.941(6)	O(3)−Cr(3)−O(4)	88.1(2)
Cr(1)−O(2)	1.937(6)	O(1)−Cr(3)−O(4)	87.8(2)
Cr(1)−O(3)	1.933(6)	O(3)−Cr(3)−O(1)	88.5(2)
Cr(2)−O(1)	1.942(6)	O(3)−Cr(4)−O(2)	88.1(2)
Cr(2)−O(2)	1.963(6)	O(3)−Cr(4)−O(4)	88.0(2)
Cr(2)−O(4)	1.946(6)	O(2)−Cr(4)−O(4)	87.6(2)
Cr(3)−O(1)	1.934(6)	Cr(3)−O(1)−Cr(1)	91.4(2)
Cr(3)−O(3)	1.931(6)	Cr(3)−O(1)−Cr(2)	92.4(2)
Cr(3)−O(4)	1.926(6)	Cr(2)−O(1)−Cr(1)	93.6(2)
Cr(4)−O(2)	1.937(6)	Cr(1)−O(2)−Cr(4)	91.8(2)
Cr(4)−O(3)	1.927(6)	Cr(1)−O(2)−Cr(2)	93.1(2)
Cr(4)−O(4)	1.933(6)	Cr(2)−O(2)−Cr(4)	92.5(2)
Cr(1)−Cp*(1)[a]	1.91(1)	Cr(1)−O(3)−Cr(4)	92.2(2)
Cr(2)−Cp*(2)[a]	1.91(1)	Cr(3)−O(3)−Cr(4)	91.9(3)
Cr(3)−Cp*(3)[a]	1.90(1)	Cr(1)−O(3)−Cr(3)	91.8(2)
Cr(4)−Cp*(4)[a]	1.91(1)	Cr(2)−O(4)−Cr(4)	93.2(2)
		Cr(3)−O(4)−Cr(4)	91.9(3)
		Cr(2)−O(4)−Cr(3)	92.6(2)

[a] Cp* is the centroid of the C_5 ring of the $(\eta\text{-}C_5Me_5)$ ligand.

controlled potential coulometry. Cyclic voltammetry gave broad peaks, which were difficult to interpret; an example, the cyclic voltammograms for $[(\eta\text{-}C_5Me_5)Cr(\mu_3\text{-}O)]_4$, is available in the Supporting Information. The differential pulse voltammogram for $[(\eta\text{-}C_5H_5)Cr(\mu_3\text{-}O)]_4$ is shown in Figure 4. There were two waves, at $E_{1/2} = +0.20$ V and $E_{1/2} = -0.11$ V (potentials are referenced to $(\eta\text{-}C_5H_5)_2Fe/(\eta\text{-}C_5H_5)_2Fe^+$, see Experimental Section), and the processes responsible for these waves were electrochemically irreversible. They were further inves-

Table 4. Distances and Angles in the tcnq Unit of 3

distance (Å)		angle (deg)	
C(50)−C(51)	1.44(1)	C(50)−C(51)−C(52)	121.7(12)
C(51)−C(52)	1.31(2)	C(51)−C(52)−C(53)	124.5(13)
C(52)−C(53)	1.41(2)	C(52)−C(53)−C(54)	114.4(12)
C(53)−C(54)	1.45(2)	C(53)−C(54)−C(55)	120.4(12)
C(54)−C(55)	1.35(2)	C(54)−C(55)−C(50)	124.1(12)
C(55)−C(50)	1.40(1)	C(55)−C(50)−C(51)	114.7(11)
C(50)−C(59)	1.41(1)	C(52)−C(53)−C(56)	124.1(14)
C(53)−C(56)	1.39(2)	C(54)−C(53)−C(56)	121.4(13)
C(56)−C(57)	1.41(2)	C(53)−C(56)−C(57)	121(2)
C(56)−C(58)	1.39(2)	C(53)−C(56)−C(58)	123(2)
C(57)−N(1)	1.14(2)	C(56)−C(57)−N(1)	174(3)
C(58)−N(2)	1.15(2)	C(56)−C(58)−N(2)	179(2)
C(59)−C(60)	1.43(2)	C(51)−C(50)−C(59)	122.6(10)
C(59)−C(61)	1.40(2)	C(55)−C(50)−C(59)	122.7(11)
C(60)−N(3)	1.15(2)	C(50)−C(59)−C(60)	120.5(12)
C(61)−N(4)	1.13(1)	C(50)−C(59)−C(61)	123.2(11)
		C(59)−C(60)−N(3)	179(2)
		C(59)−C(61)−N(4)	179(2)

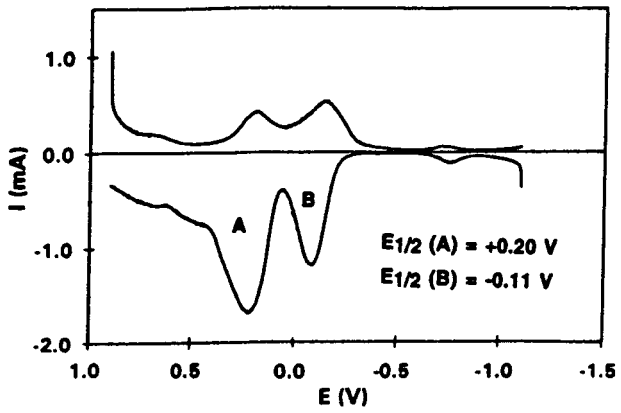

Figure 4. Differential pulse voltammogram for $[(\eta\text{-}C_5H_5)\text{-}Cr(\mu_3\text{-}O)]_4$. The pulse height was 25 mV, the scan rate 25 mV s^{-1}, the scan increment 2 mV, and the step time 0.08 s.

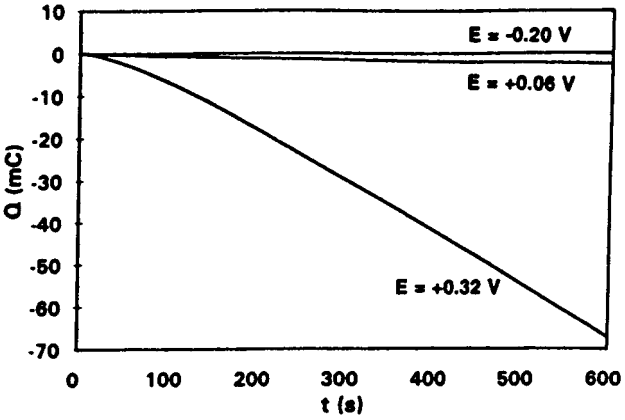

Figure 5. Controlled potential coulomogram for $[(\eta\text{-}C_5H_5)\text{-}Cr(\mu_3\text{-}O)]_4$.

tigated by controlled potential coulometry, as shown in Figure 5. At an applied potential of +0.32 V, a more positive potential than the wave at +0.20 V, there was a high current, but at an applied potential of +0.06 V, in the valley between the waves, there was no current. At −0.20 V, a more negative potential than the wave at −0.11 V, there was only a very low current, which was ascribed to electrolysis of impurities or of the $LiAsF_6$/thf electrolyte. Thus the wave at +0.20 V was

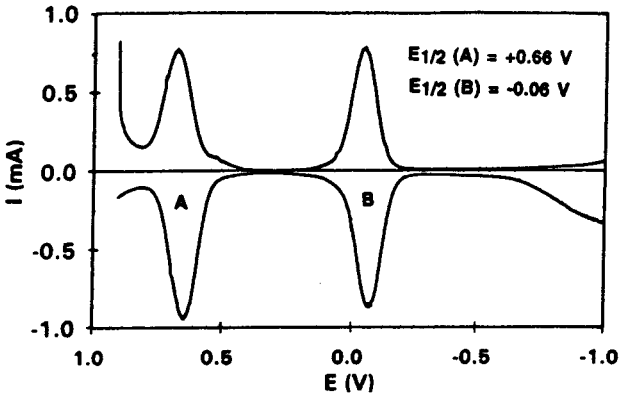

Figure 6. Differential pulse voltammogram for $[(\eta\text{-}C_5Me_5)\text{-}Cr(\mu_3\text{-}O)]_4$. The pulse height was 25 mV, the scan rate 20 mV s^{-1}, the scan increment 2 mV, and the step time 0.1 s.

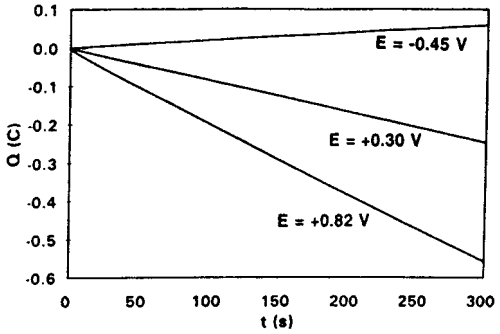

Figure 7. Controlled potential coulomogram for $[(\eta\text{-}C_5Me_5)Cr(\mu_3\text{-}O)]_4$.

ascribed to one-electron oxidation of $[(\eta\text{-}C_5H_5)Cr(\mu_3\text{-}O)]_4$ (eq 1); that at −0.11 V to one-electron reduction (eq 2).

$$[(\eta\text{-}C_5H_5)Cr(\mu_3\text{-}O)]_4 \rightarrow \{[(\eta\text{-}C_5H_5)Cr(\mu_3\text{-}O)]_4\}^+ + e^- \quad (1)$$

$$[(\eta\text{-}C_5H_5)Cr(\mu_3\text{-}O)]_4 + e^- \rightarrow \{[(\eta\text{-}C_5H_5)Cr(\mu_3\text{-}O)]_4\}^- \quad (2)$$

The differential pulse voltammogram of $[(\eta\text{-}C_5Me_5)\text{-}Cr(\mu_3\text{-}O)]_4$ is shown in Figure 6. There were two peaks, at $E_{1/2} = +0.66$ V and $E_{1/2} = -0.06$ V, both due to electrochemically reversible processes. The relative slope of the current/time curves observed by controlled potential coulometry at +0.30 and +0.82 V was 2.02, as shown in Figure 7. This definitively established that the peak at −0.06 V represented a one-electron oxidation to the monocation (eq 3), and the peak at +0.66 V represented a further one-electron oxidation to the dication (eq 4), both reactions being reversible.

$$[(\eta\text{-}C_5Me_5)Cr(\mu_3\text{-}O)]_4 = \{[(\eta\text{-}C_5Me_5)Cr(\mu_3\text{-}O)]_4\}^+ + e^- \quad (3)$$

$$\{[(\eta\text{-}C_5Me_5)Cr(\mu_3\text{-}O)]_4\}^+ = \{[(\eta\text{-}C_5Me_5)Cr(\mu_3\text{-}O)]_4\}^{2+} + e^- \quad (4)$$

The electrochemical oxidation of $[(\eta\text{-}C_5H_4Me)Cr(\mu_3\text{-}A)]_4$ (A = O, S, Se) was investigated previously by Green and co-workers, using cyclic voltammetry.[17] It was

(17) Davies, C. E.; Green, J. C.; Kaltsoyannis, N.; MacDonald, M. A.; Qin, J.; Rauchfuss, T. B.; Redfern, C. M.; Stringer, G. H.; Woolhouse, M. G. *J. Chem. Soc., Dalton Trans.* **1992**, 3779.

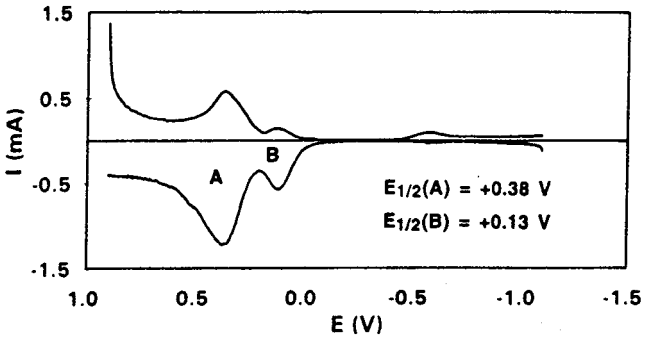

Figure 8. Differential pulse voltammogram for [(η-C_5H_4Me)Cr(μ_3-O)]$_4$. The pulse height was 25 mV, the scan rate 50 mV s^{-1}, the scan increment 5 mV, and the step time 0.1 s.

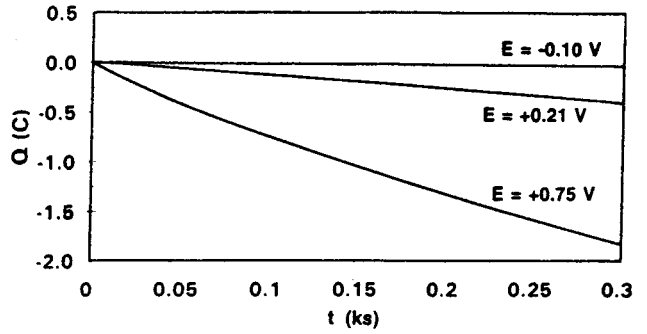

Figure 9. Controlled potential coulomogram for [(η-C_5H_4Me)Cr(μ_3-O)]$_4$.

Table 5. Electrode Potentials for the Formation of {[(η-C_5R_5)Cr(μ_3-O)]$_4$}$^{n+}$ from [(η-C_5R_5)Cr(μ_3-O)]$_4$

{[(η-C_5R_5)Cr(μ_3-O)]$_4$}$^{n+}$	$n = -1$	$n = 1$	$n = 2$
R = H	−0.11[a]	0.20	
R_5 = H_4Me		0.13	0.38
R = Me		−0.06	0.66

[a] $E_{1/2}$ (V) versus the (η-C_5H_5)$_2$Fe/(η-C_5H_5)$_2$Fe$^+$ couple.

concluded that [(η-C_5H_4Me)Cr(μ_3-O)]$_4$ underwent a reversible one-electron oxidation to the monocation and a further irreversible one-electron oxidation to the dication. Since the experimental conditions were different from those used in the present work, the electrochemistry of [(η-C_5H_4Me)Cr(μ_3-O)]$_4$ was reinvestigated. The differential pulse voltammogram for [(η-C_5H_4Me)Cr(μ_3-O)]$_4$ is shown in Figure 8. It is similar in form to that of [(η-C_5H_5)Cr(μ_3-O)]$_4$, shown in Figure 4, with two peaks at $E_{1/2}$ = +0.38 V and $E_{1/2}$ = +0.13 V, both due to electrochemically irreversible processes. However, the controlled potential coulomogram (Figure 9) showed that there were two consecutive processes, as for [(η-C_5Me_5)Cr(μ_3-O)]$_4$. Because the peaks for [(η-C_5H_4Me)Cr(μ_3-O)]$_4$ overlap, it was not possible to obtain independent current/time curves by controlled potential coulometry (the ratio of the slopes was 4.9). However, it was clear that the two peaks were due to successive oxidation, as proposed by Green and co-workers,[17] although we found that both oxidation processes were irreversible.

The results of the electrochemical experiments on [(η-C_5R_5)Cr(μ_3-O)]$_4$ are summarized in Table 5. It is seen that the oxidation of [(η-C_5R_5)Cr(μ_3-O)]$_4$ to {[(η-C_5R_5)Cr(μ_3-O)]$_4$}$^+$ was progressively easier as the number of methyl groups on the cyclopentadienyl ligand increased, which is in agreement with the donor capacity of (η-C_5R_5): R_5 = H_5 < MeH_4 < Me_5. However, it is surprising that the presence of even one methyl group on the cyclopentadienyl ligand makes it possible to further oxidize {[(η-C_5R_5)Cr(μ_3-O)]$_4$}$^+$ to {[(η-C_5R_5)Cr(μ_3-O)]$_4$}$^{2+}$ when R_5 = H_4Me or Me_5.

Preparation and Characterization of 2 and 3. When a solution of [(η-C_5H_5)Cr(μ_3-O)]$_4$ and $LiAsF_6$ in tetrahydrofuran was electrolyzed at an applied potential of +0.32 V, the current flow decreased to zero after 11 h, but only 50% of the theoretical coulombs had been consumed. Addition of ether to the solution precipitated an intimate mixture of un-oxidized [(η-C_5H_5)Cr(μ_3-O)]$_4$, {[(η-C_5H_5)Cr(μ_3-O)]$_4$}{AsF_6}, and {Li(thf)$_4$}{AsF_6}, as shown by analysis and X-ray diffraction. Chemical oxidation of [(η-C_5H_5)Cr(μ_3-O)]$_4$ with $AgBF_4$ also produced an inseparable mixture of [(η-C_5H_5)Cr(μ_3-O)]$_4$ and {[(η-C_5H_5)Cr(μ_3-O)]$_4$}{BF_4}.

Oxidation of blue [(η-C_5Me_5)Cr(μ_3-O)]$_4$ with $AgBF_4$ in tetrahydrofuran solution gave deep purple {[(η-C_5Me_5)Cr(μ_3-O)]$_4$}{BF_4} in 48% yield after crystallization. The product was formulated as a 1:1 salt on the basis of microanalysis and X-ray diffraction. Reaction of [(η-C_5Me_5)Cr(μ_3-O)]$_4$ with tcnq in tetrahydrofuran solution gave dark green {[(η-C_5Me_5)Cr(μ_3-O)]$_4$}{tcnq} in 64% yield after crystallization. The crystal structure showed that the product also had a 1:1 relationship of {[(η-C_5Me_5)Cr(μ_3-O)]$_4$} to {tcnq}, but this did not determine the degree of charge transfer. The relation between the number and frequencies of the ν(CN) vibrations and the charge on tcnq in salts containing d-block metal complexes was discussed by Murphy and O'Hare,[18] and a graphical relation between ν(CN) and the charge on tcnq in a variety of compounds was presented by Bloch and co-workers.[19] The ν(CN) frequencies for {[(η-C_5Me_5)Cr(μ_3-O)]$_4$}{tcnq} were 2150 cm^{-1} (m) and 2175 cm^{-1} (s), identical to those found for {Fe(η^5-C_9Me_7)$_2$}{tcnq), which is a 1:1 salt,[18] whereas for tcnq the ν(CN) frequency was 2220 cm^{-1} (m) (lit.[18] 2222 cm^{-1} (m), 2226 cm^{-1}). The graphical relation of Bloch and co-workers[19] suggested that the charge on the tcnq of {[(η-C_5Me_5)Cr(μ_3-O)]$_4$}{tcnq} was −1.02 and therefore that the compound was a 1:1 salt. Kistenmacher and co-workers developed a relationship between the charge on tcnq and the distances b, c, and d, defined in Figure 3 and listed in Table 6.[20,21] This relationship suggests that the charge on the tcnq of {[(η-C_5Me_5)Cr(μ_3-O)]$_4$}{tcnq} was −0.78. The charge on the tcnq of {Fe(η^5-C_9Me_7)$_2$}{tcnq), determined by the Kistenmacher relationship, was −1.30, compared to −1.02 calculated from the frequency of ν(CN). It is possible that the relatively large errors in the tcnq distances of {[(η-C_5Me_5)Cr(μ_3-O)]$_4$}{tcnq} are responsible for the low calculated charge.

Structure of the Salts 2 and 3 and the Geometry of the {[(η-C_5Me_5)Cr(μ_3-O)]$_4$}$^+$ Unit, as Determined by X-ray Diffraction. The salts **2** and **3** consist of {[(η-C_5Me_5)Cr(μ_3-O)]$_4$}$^+$ cations and {BF_4}$^-$ or {tcnq}$^-$

(18) Murphy, U. J.; O'Hare, D. *Inorg. Chem.* **1994**, *33*, 1833.
(19) Chappell, J. S.; Bloch, A. N.; Bryden, W. A.; Maxfield, M.; Poehler, T. O.; Cowan, D. O. *J. Am. Chem. Soc.* **1981**, *103*, 2443.
(20) Kistenmacher, T. J.; Emge, T. J.; Bloch, A. N.; Cowan, D. O. *Acta Crystallogr.* **1982**, *B38*, 1193.
(21) Le Stang, S.; Conan, F.; Sala Pala, J.; Le Mest, Y.; Garland, M.-T.; Baggio, R.; Faulques, E.; Leblanc, A.; Molinié, P.; Toupet, L. *J. Chem. Soc., Dalton Trans.* **1998**, 489.

Table 6. Degree of Charge Transfer in tcnq Compounds

compound	distance (Å) a[b]	b[b]	c[b]	d[b]	c/(b + d)	charge[a] (ρ)	ref
tcnq	1.346(3)	1.448(4)	1.374(3)	1.441(3)	0.476	0.00[14]	22
Rb{tcnq}	1.373(1)	1.423(3)	1.420(1)	1.416(8)	0.500	−1.00[c]	23
{W(S_2CNMe_2)$_4$}{tcnq}	1.365(7)	1.408(7)	1.431(9)	1.418(9)	0.506	−1.26	21
{Fe(η^5-C_9Me_7)$_2$}{tcnq)	1.38(1)	1.41(1)	1.43(1)	1.41(1)	0.507	−1.30	18
{tmtsf}{tcnq}[15]	1.354(6)	1.438(6)	1.375(6)	1.429(6)	0.480	−0.17	20
{[(η-C_5Me_5)Cr(μ_3-O)]$_4$}{tcnq}	1.33(2)	1.42(2)	1.40(2)	1.41(2)	0.495	−0.78	this work

[a] Predicted by the Kistenmacher relationship: $\rho = -41.667[c/(b + d)] + 19.833$.[20] [b] The distances a, b, c, and d are defined in Figure 3. [c] By definition. [e] tmtsf = 4,4′,5,5′-tetramethyl-$\Delta^{2,2'}$-bi-1,3-selenole.[20]

Table 7. Comparison of M−M Distances (Å) in {[(η-C_5R_5)M(μ_3-A)]$_4$}$^{n+}$ Clusters

{[(η-C_5R_5)M(μ_3-A)]$_4$}$^{n+}$	cluster electrons	M−M	symmetry	average M−M	ref
[(η-C_5H_5)Cr(μ_3-O)]$_4$	12	2.71 [2], 2.82 [2], 2.90 [2][a]	D_2	2.81	9
[(η-C_5H_4Me)Cr(μ_3-O)]$_4$	12	2.76 [4], 2.90 [2]	D_{2d}	2.80	11
[(η-C_5Me_5)Cr(μ_3-O)]$_4$	12	2.83 [6]	T_d	2.83	7
{[(η-C_5Me_5)Cr(μ_3-O)]$_4$}$^+$	11	2.81 [4], 2.78 [2]	D_{2d}	2.80	this work
	11	2.78 [3], 2.82 [3]	C_{3v}	2.80	this work
(η-C_5H_4Me)$_2$(η-C_5Me_5)$_2$[Mo(μ_3-S)]$_4$	12	2.90 [6]	T_d	2.90	26
[(η-$C_5H_4Pr^i$)Mo(μ_3-S)]$_4$	12	2.89, 2.90 [3], 2.91 [2]	$\sim T_d$	2.90	27
{[(η-$C_5H_4Pr^i$)Mo(μ_3-S)]}$^+$	11	2.86, 2.89 [2], 2.90 [2], 2.92	$\sim T_d$	2.89	27
{[(η-$C_5H_4Pr^i$)Mo(μ_3-S)]}$^{2+}$	10	2.79, 2.82, 2.86, 2.88, 2.90 [2]	$\sim T_d$	2.86	27
[(η-C_5H_5)V(μ_3-S)]	8	2.85 [2], 2.87 [2], 2.90 [2]	D_2	2.88	28
[(η-C_5H_4Me)V(μ_3-S)]	8	2.87 [4], 2.88 [2]	D_{2d}	2.87	29
		2.86 [4], 2.87 [2]	$\sim T_d$	2.87	30
{[(η-C_5H_4Me)V(μ_3-S)]}$^+$	7	2.85 [6]	T_d	2.85	29
[(η-C_5H_5)Fe(μ_3-S)]	20	2.65 [2], 3.36 [4]	D_{2d}	3.12	31
		2.63 [2], 3.37 [4]	D_{2d}	3.12	32
[(η-C_5H_4Me)Fe(μ_3-S)]	20	2.61 [2], 3.36 [2], 3.39 [2]	D_{2d}	3.12	33
{[(η-C_5H_5)Fe(μ_3-S)]}$^+$	19	2.65 [2], 3.19 [2], 3.32 [2]	D_2	3.05	34
		2.66 [2], 3.19 [2], 3.30 [2]	D_2	3.05	35
		2.63 [2], 3.21 [2], 3.30 [2]	D_2	3.05	35
{[(η-C_5H_4Me)Fe(μ_3-S)]}$^+$	19	2.90 [4], 3.30 [2]	D_{2d}	3.03	33
{[(η-C_5H_5)Fe(μ_3-S)]}$^{2+}$	18	2.83 [4], 3.25 [2]	D_{2d}	2.97	36
[(η-C_5H_5)Fe(μ_3-Se)]	20	2.72 [2], 3.56 [4]	D_{2d}	3.29	37
{[(η-C_5H_5)Fe(μ_3-Se)]}$^+$	19	2.72 [2], 3.36−3.48 [4]	C_2	3.20	37
{[(η-C_5H_5)Fe(μ_3-Se)]}$^{2+}$	18	2.95 [4], 3.42 [2]	D_{2d}	3.11	37
{[(η-C_5H_5)Fe(μ_3-Se)]}$^{3+}$	17	2.78, 2.80, 2.84, 2.93, 3.36 [2]	C_2 ($\sim D_{2d}$)	3.01	38
[(η-C_5H_5)Co(μ_3-S)]	24	3.24 [2], 3.32, 3.30, 3.34 [2]	C_2 ($\sim D_{2d}$)	3.29	39
{[(η-C_5H_5)Co(μ_3-S)]}$^+$	23	3.17 [4], 3.33 [2]	D_{2d}	3.22	39

[a] Reference 24.

anions. In **2**, the shortest H(methyl)−F distance is 2.44 Å and the shortest C(methyl)−F is 3.31 Å. In **3**, the shortest H(methyl)−N distance in **3** is 2.58 Å and the shortest C(methyl)−N is 3.50 Å. The shortest distance between nitrogen atoms of tcnq units, which represents the separation between {tcnq}$^-$ anions, is 3.54 Å.

The important distances and angles in the {[(η-C_5Me_5)Cr(μ_3-O)]$_4$}$^+$ unit of **2** and **3** are given in Tables 2 and 3, respectively. The {[(η-C_5Me_5)Cr(μ_3-O)]$_4$} unit of **2** has exact D_{2d} symmetry, the S_4 axis being a result of the tetragonal $I\bar{4}$ space group symmetry. The Cr−Cr distances in **2** are 2.815(2) Å [4][24] and 2.781(2) Å [2]; the Cr−O distances average 1.943(5,2) Å [4] and 1.927(5) Å [2];[25] the Cr−O−Cr angles average 93.0(2,3)° [4] and 91.9(2)° [2]; and the O−Cr−O angles average 86.9(2,2)° [4] and 87.9(2)° [2]. The {[(η-C_5Me_5)Cr(μ_3-O)]$_4$}$^+$ unit of **3** has approximately C_{3v} symmetry, with Cr(2) being the apical chromium atom. The averages of the Cr(2)−Cr and Cr(2)−O distances are 2.816(2,18) and 1.950(6,13) Å, respectively, whereas the averages of the other Cr−Cr and Cr−O distances are 2.776(2,5) and 1.933(6,7) Å. The O−Cr(2)−O angles average 86.6(2,3)°, whereas the average of the other O−Cr−O angles is 87.9(2,9)°. The neutral cluster **1** has approximately T_d symmetry, with average Cr−Cr and Cr−O distances of 2.834(2,6) and 1.945(5,25) Å, respectively.[7] Table 7 lists the M−M distances and symmetry in {[(η-C_5R_5)M(μ_3-A)]$_4$}$^{n+}$ clusters for which both neutral and cationic forms are known. It is seen from this table that those clusters with 12 or fewer electrons often exhibit small distortions (<0.15 Å) from T_d symmetry that are apparently dependent on the R group of the (η-C_5R_5) ligand. Clusters with more than 12 electrons often have large distortions (0.40−0.85 Å) from T_d symmetry, and the distortions are dependent on n and on the identity of atom A.

The small distortions from T_d symmetry in the [M(μ_3-A)]$_4$ units of {[(η-C_5R_5)M(μ_3-A)]$_4$}$^{n+}$ clusters having less than 12 electrons were previously ascribed to packing forces.[7,9,26,33] However, recent calculations by McGrady, using broken-symmetry density functional theory (DFT),

(22) Long, R. E.; Sparks, R. A.; Trueblood, K. N. *Acta Crystallogr.* **1965**, *18*, 932.
(23) Hoekstra, A.; Spoelder, T.; Vos, A. *Acta Crystallogr.* **1972**, *B28*, 14.
(24) The numeral in square brackets is the number of M−M distances.
(25) The first numeral in brackets is the estimated standard deviation; the second is the maximum deviation from the average.
(26) Williams, P. D.; Curtis, M. D. *Inorg. Chem.* **1986**, *25*, 4562.
(27) Bandy, J. A.; Davies, C. E.; Green, J. C.; Green, M. L. H.; Prout, K.; Rodgers, D. P. S. *J. Chem. Soc., Chem. Commun.* **1983**, 1395.
(28) Duraj, S. A.; Andras, M. T.; Rihter, B. *Polyhedron* **1989**, *8*, 2763.

Table 8. Comparison of Distances (Å) and Angles (deg) in the {[(η-C_5Me_5)Cr(μ_3-O)]$_4$} Unit of 1, 2, and 3

	1	2	3
Cr−Cr	2.834(2, 6)[25]	2.804(2, 23)	2.796(2, 35)
Cr−O	1.945(5, 25)	1.938(5, 11)	1.937(6, 11)
Cr−C	2.270(8, 22)	2.257(8, 29)	2.24(1, 3)
Cr−Cp*	1.932(8, 13)	1.909(8)	1.91(1, 1)
O−Cr−O	86.4(2, 9)	87.3(2, 6)	87.6(2, 13)
Cr−O−Cr	93.5(2, 12)	92.7(2, 7)	92.7(2, 13)

[a] Reference 25.

indicated that the ground state of [(η-C_5H_5)Cr(μ_3-O)]$_4$ was a rhombically distorted tetrahedron of D_{2d} symmetry with two long and four short Cr−Cr distances.[40] The undistorted (T_d) and twisted (D_2) structures were calculated to be only 10−12 kJ mol^{-1} higher in energy and the electronic driving force for the rhombic distortion was of similar magnitude to intra- or intermolecular steric interactions.[40] The steric bulk of η-C_5Me_5 would favor a symmetrical T_d arrangement for the [(η-C_5Me_5)-Cr(μ_3-O)]$_4$ unit of **1**, **2**, or **3**, and therefore it is not clear why the small distortions, to D_{2d} with two short and four long Cr−Cr distances in **2** and to C_{3v} in **3**, occur.

The distances and angles in the [(η-C_5Me_5)Cr(μ_3-O)]$_4$ units of **1**, **2**, and **3** are compared in Table 8, from which it is seen that the average distances for **2** and **3** were identical within experimental error. However, the Cr−Cr, Cr−O, and Cr−Cp* distances in **2** and **3** were 0.034-(2), 0.007(5), and 0.02(1) Å shorter than those in **1**, respectively. There are corresponding changes in the O−Cr−O and Cr−O−Cr angles. It is seen from Table 7 that there is a similar ∼0.03 Å contraction of the M_4 tetrahedron with each unit increase in the positive charge for other {[(η-C_5R_5)M(μ_3-A)]$_4$}$^{n+}$ clusters with less than 12 electrons. Clusters with more than 12 electrons show a larger (0.06−0.09 Å) contraction of the M_4 tetrahedron as the positive charge increases. The DFT calculations showed that the 12 cluster electrons of [(η-C_5R_5)Cr(μ_3-O)]$_4$ were not delocalized over the four chromium atoms,[40] in contradiction to the previous models, which were based on calculations of the extended Hückel type.[9,26,36,41] According to the DFT model, the electronic structure of [(η-C_5R_5)Cr(μ_3-O)]$_4$ is best derived from the interaction of four Cr(III), d^3 (S = 3/2) ions, rather than from the perturbation of six Cr−Cr bonds. The shortening of the Cr−Cr, Cr−O, and Cr−Cp* distances in **2** and **3** compared to **1** is due to the increase in the positive charge and not to a change in the degree of Cr−Cr bonding.

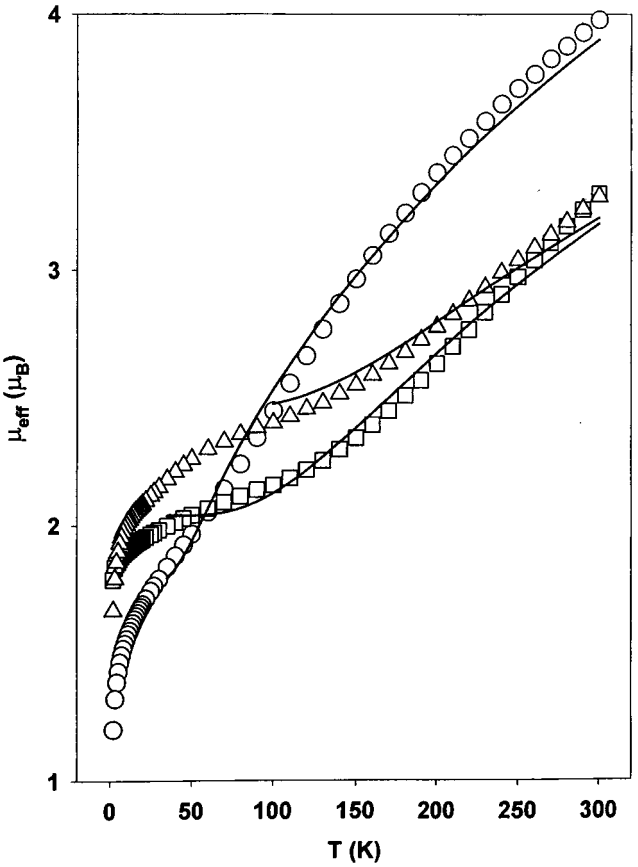

Figure 10. Magnetic behavior of **1** (circles), **2** (squares), and **3** (triangles) over the temperature range 2−300 K. Lines are calculated from theory, as described in the text.

Magnetism of {[(η-C_5Me_5)Cr(μ_3-O)]$_4$}$^{n+}$ (n = 0, 1). The ^{1}H NMR spectrum of **2**, in C^2HCl_3 solution, showed a single broad signal at −3.08 ppm ($\Delta\nu_{1/2}$ = 24.1 Hz), assigned to the protons of the η-C_5Me_5 ligand. The signal for **3** was at −3.16 ppm ($\Delta\nu_{1/2}$ = 34.8 Hz). These signals may be compared to that of **1**: 2.14 ppm ($\Delta\nu_{1/2}$ = 124.9 Hz).[7] They are typical of compounds with magnetic moments. The line width suggested that {[(η-C_5Me_5)-Cr(μ_3-O)]$_4$}$^+$ had a lower magnetic moment than [(η-C_5-Me_5)Cr(μ_3-O)]$_4$ at room temperature.

The EPR spectrum of **1**, in tetrahydrofuran solution, showed a very broad featureless signal at both 295 and 80 K. The salt **2** was EPR silent at room temperature, again in tetrahydrofuran solution. These results indicated the presence of more than one unpaired electron in these clusters. The EPR spectrum of **3** in tetrahydrofuran solution, showed a multiplet at g = 2.002, which was assigned to {tcnq}$^-$. There was no signal assignable to {[(η-C_5Me_5)Cr(μ_3-O)]$_4$}$^+$. The EPR spectrum of powdered samples of **3** showed a signal at g = 2.0023 ($\Delta\nu_{1/2} \approx$ 3 G) with no hyperfine splitting, at 295 and 120 K.

Magnetism of {[(η-C_5Me_5)Cr(μ_3-O)]$_4$}{BF_4} (2). The magnetic moment of **2**, calculated per mole of [(η-C_5Me_5)Cr(μ_3-O)]$_4$, is plotted versus temperature in Figure 10. The moment decreased from 3.30 μ_B to 1.79 μ_B as the temperature decreased from 300 to 2 K, which

(29) Darkwa, J.; Lockemeyer, J. R.; Boyd, P. D. W.; Rauchfuss, T. B.; Rheingold, A. L. *J. Am. Chem. Soc.* **1988**, *110*, 141.
(30) Pasynskii, A. A.; Eremenko, I. L.; Katugin, A. S.; Gasanov, G. Sh. Turchanova, E. A.; Ellert, O. G.; Shklover, V. E.; Struchkov, Yu. T.; Berberova, N. T.; Sogomonova, A. G.; Okhlobystin, O. Yu. *J. Organomet. Chem.* **1988**, *344*, 195.
(31) Wei, C. H.; Wilkes, G. R.; Treichel, P. M.; Dahl, L. F. *Inorg. Chem.* **1966**, *5*, 900.
(32) Schunn, R. A.; Fritchie, C. J.; Prewitt, C. T. *Inorg. Chem.* **1966**, *5*, 892.
(33) Blonk, H. L.; van der Linden, J. G. M.; Steggerda, J. J.; Geleyn, R. P.; Smits, J. M. M.; Beurskens, G.; Beurskens, P. T.; Jordanov, J. *Inorg. Chem.* **1992**, *31*, 957.
(34) Trinh-Toan; Fehlhammer, W. P.; Dahl, L. F. *J. Am. Chem. Soc.* **1977**, *99*, 402.
(35) Shimoi, M.; Satoh, A.; Ogino, H. *Bull. Chem. Soc. Jpn.* **1991**, *64*, 11.
(36) Trinh-Toan; Teo, B. K.; Ferguson, J. A.; Meyer, T. J.; Dahl, L. F. *J. Am. Chem. Soc.* **1977**, *99*, 408.
(37) See ref 33, Table 6.
(38) Ogino, H.; Tobita, H.; Yanigasawa, K.; Shimoi, M.; Kabuto, C. *J. Am. Chem. Soc.* **1987**, *109*, 5847.
(39) Simon, G. L.; Dahl, L. F. *J. Am. Chem. Soc.* **1973**, *95*, 2164.
(40) McGrady, J. E. *J. Chem. Soc., Dalton Trans.* **1999**, 1393.
(41) Bottomley, F.; Grein, F. *Inorg. Chem.* **1982**, *21*, 4170.

is consistent with antiferromagnetism. The value at 2 K is in agreement with complete intracluster coupling of the 11 electrons of the $\{[(\eta\text{-}C_5Me_5)Cr(\mu_3\text{-}O)]_4\}^+$ unit of **2**, yielding a $S = 1/2$ ground state with $g = 2$. The only model presently available for the magnetic behavior of cubane-like clusters such as $\{[(\eta\text{-}C_5Me_5)Cr(\mu_3\text{-}O)]_4\}^+$ assumes the antiferromagnetic interaction of localized spins on four metal centers that are arranged tetrahedrally,[42] as in the DFT model.[40] There are three Cr^{III} and one Cr^{IV} in the present case. The Hamiltonian describing the interaction of the four metal centers is given in eq 5, in which $S_A = S_B = S_C = 3/2$ and $S_D = 1$, J is the interaction parameter between two $S = 3/2$ centers, and J' is the interaction parameter between $S = 3/2$ and $S = 1$ centers. The relative energies of the eigenstates for this system are given in eq 6, in which $S_{AB} = S_A + S_B$, $S_{ABC} = S_A + S_B + S_C$, and $S = S_{ABC} + S_D$.[42]

$$H = -J(S_A \cdot S_B + S_B \cdot S_c + S_A \cdot S_C) - J' \cdot S_D(S_A + S_B + S_C) \quad (5)$$

$$E(S,S_{ABC},S_{AB}) = [(J - J')/2][S_{ABC}(S_{ABC} + 1)] - [J'/2][S(S + 1)] \quad (6)$$

The susceptibilities were calculated as a function of temperature and of the parameters g, J, and J' by incorporating the energies into the Van Vleck equation.[43] The experimental and calculated susceptibilities were fitted using a nonlinear least-squares procedure, minimizing the goodness of fit function F, which is defined in eq 7. In the fitting procedure, g was fixed at

$$F = [1/n\sum_{i=1}^{n}((\chi_i^{obs} - \chi_i^{calc})^2(\chi_i^{obs})^{-2})]^{0.5} \quad (7)$$

2, J and J' were variables, and a variable parameter P was included, to accommodate a small amount of a paramagnetic impurity.[44] The impurity was presumed to be Curie-law Cr^{III} with $S = 3/2$ and $g = 2$. A satisfactory fit of the experimental and calculated data between 35 and 300 K was achieved. The least-squares procedure consistently gave the same value for J and J'. Thus the data did not distinguish between J and J', and only an average J was measurable. The best-fit parameters were $J = -211(34)$ cm^{-1} and $P = 0.020$, giving $F = 0.034$. A visual comparison of the experimental and calculated moments using the best-fit parameters is shown in Figure 10. Numerous attempts to fit the data between 2 and 35 K were unsuccessful, mainly because of the sharp decrease in the moment below 35 K. This may arise from zero-field splitting effects associated with the paramagnetic impurity or the presence of weak intercluster antiferromagnetic exchange.

Magnetism of $\{[(\eta\text{-}C_5Me_5)Cr(\mu_3\text{-}O)]_4\}\{tcnq\}$ (3). The magnetic moment of **3**, calculated per mole of **3**, is plotted versus temperature in Figure 10. There was a gradual decrease in the moment, from 3.29 μ_B at 300 K to 2.45 μ_B at 110 K, then a rapid decrease to 1.67 μ_B at 2 K. The experimental and calculated susceptibilities were fitted over the temperature range 100−300 K by a procedure similar to that described above for **2**, with the addition of a term for $\{tcnq\}^-$ ($S = 1/2$). Preliminary cycles showed that the paramagnetic impurity parameter was negative, and therefore P was set to zero, with $g = 2$ as before. The best-fit value obtained was $J = -266(46)$ cm^{-1} ($F = 0.036$). A visual comparison of the experimental and calculated moments using the best-fit parameters is shown in Figure 10. The data over the temperature range 2−100 K could not be fitted by the above or any other parameters.

The lowest moment observed for **3** was 1.67 μ_B at 2 K. Intracluster antiferromagnetic coupling of the 11 electrons in the $\{[(\eta\text{-}C_5Me_5)Cr(\mu_3\text{-}O)]_4\}^+$ unit of **3** would give an $S = 1/2$ ground state (as observed for **2**) and $\{tcnq\}^-$ would also have an $S = 1/2$ ground state. Therefore, the lowest value of the magnetic moment should be 2.45 μ_B, assuming no coupling between the two $S = 1/2$ species. This is in fact the value observed at 110 K, the temperature below which the model failed. The only explanation for this result is inter-ion antiferromagnetic coupling between an unpaired electron on the $\{[(\eta\text{-}C_5Me_5)Cr(\mu_3\text{-}O)]_4\}^+$ unit and one on the $\{tcnq\}^-$ of **3**.

Magnetism of $[(\eta\text{-}C_5Me_5)Cr(\mu_3\text{-}O)]_4$ (1). We reexamined the magnetic properties of **1**,[7] for comparison with the results for **2** and **3**. The results are shown in Figure 10. Intracluster antiferromagnetic coupling of the 12 cluster electrons in $[(\eta\text{-}C_5Me_5)Cr(\mu_3\text{-}O)]_4$ should result in an $S = 0$ ground state, in which case the eigenstates are given by eq 8 and the relative energies by eq 9, in which $S = S_A + S_B + S_C + S_D$.[42]

$$H = -J(S_A \cdot S_B + S_B \cdot S_c + S_A \cdot S_D + S_B S_C + S_B S_D + S_C S_D) \quad (8)$$

$$E(S) = [-J/2][S(S + 1)/2] \quad (9)$$

The data between 35 and 300 K could be fitted to this model, with the inclusion of a paramagnetic impurity as described for **2** above. The best-fit parameters obtained were $J = -262(23)$ cm^{-1} and $P = 0.051$, with g fixed at 2, giving $F = 0.040$. A visual comparison of the experimental and calculated moments using the best-fit parameters is shown in Figure 10. Once again, no fit could be found for the low-temperature data (2−35 K). The lowest observed moment for **1** was 1.20 μ_B at 2 K, compared to the expected value of zero. It cannot be established whether the magnetic behavior below 35 K arises from zero-field splitting effects associated with the paramagnetic impurity or weak intercluster antiferromagnetic exchange as in **2**. The intracluster exchange coupling constants, J, are the same, within experimental error, for **1**, **2**, and **3** (−262(23), −211(34), and −266(46) cm^{-1}, respectively). This indicates that the model of localized spins on four metal centers that are arranged tetrahedrally[40,42] is essentially correct. Small differences in symmetry or in the Cr−Cr distances have little affect on the intracluster interaction. The J values are of a relatively high magnitude for oxo-bridged Cr(III) compounds. It was estimated that J for $\{[(2\text{-picetam})_2Cr(\mu\text{-}O)]_2\}^{2+}$ (picetam = (2-pyridyl)ethylamine) was −83 cm^{-1},[45] and J values ranging from −6

(42) Kahn, O. *Molecular Magnetism*; VCH Publishers Inc.: New York, 1993.
(43) Van Vleck, J. H. *Electric and Magnetic Susceptibilities*; Oxford University Press: Oxford and New York, 1932.
(44) Ehlert, M. K.; Storr, A.; Thompson, R. C. *Can. J. Chem.* **1993**, *71*, 1412.

to −62 cm^{-1} were given for 10 compounds containing the $\{[O_4Cr(\mu\text{-}O)]_2\}^{14-}$ unit, with the stronger antiferromagnetic interactions associated with smaller Cr−O−Cr angles.[46] All these compounds contain two octahedrally coordinated Cr(III) centers bridged by two μ_2-oxide ions, whereas $\{[(\eta\text{-}C_5Me_5)Cr(\mu_3\text{-}O)]_4\}$ contain three octahedrally coordinated Cr(III) centers bridged by one μ_3-oxide ion.

Conclusions

Oxidation of $[(\eta\text{-}C_5Me_5)Cr(\mu_3\text{-}O)]_4$ (**1**) by $AgBF_4$ or tcnq gave $\{[(\eta\text{-}C_5Me_5)Cr(\mu_3\text{-}O)]_4\}\{BF_4\}$ (**2**) or $\{[(\eta\text{-}C_5Me_5)Cr(\mu_3\text{-}O)]_4\}\{tcnq\}$ (**3**), respectively. It was shown by X-ray diffraction that the average Cr−Cr, Cr−O, and Cr−Cp* distances in **2** and **3** were 0.034(2), 0.007(5), and 0.02(1) Å, respectively, shorter than those in **1**. All three compounds were antiferromagnetic, with similar intracluster exchange coupling constants, J (−211 to −266 cm^{-1}). The magnetic data for **3** suggested that there was coupling between an unpaired electron on $\{[(\eta\text{-}C_5Me_5)Cr(\mu_3\text{-}O)]_4\}^+$ and one on $\{tcnq\}^-$ at temperatures below 110 K.

Acknowledgment. We thank Professor T. Stanley Cameron (Dalhousie University) for collecting the X-ray diffraction data, Dr. Gilles Villemure (UNB) for assistance with the electrochemical measurements, Dr. F. G. Herring (UBC) for the EPR spectra of **3** at low temperatures, and Tara-Lee Tracy for the preparation of $[(\eta\text{-}C_5H_4Me)Cr(\mu_3\text{-}O)]_4$. We are grateful to the Natural Sciences and Engineering Research Council of Canada for financial support of this work.

Supporting Information Available: Current/voltage plots for $[(\eta\text{-}C_5R_5)Cr(\mu_3\text{-}O)]_4$; tables of crystallographic data, atom coordinates, thermal parameters, and distances and angles for $\{[(\eta\text{-}C_5Me_5)Cr(\mu_3\text{-}O)]_4\}\{BF_4\}$ and $\{[(\eta\text{-}C_5Me_5)Cr(\mu_3\text{-}O)]_4\}\{tcnq\}(thf)_{0.5}$. This material is available free of charge via the Internet at http://pubs.acs.org.

OM001067Y

(45) Michelsen, M.; Pedersen, E.; Wilson, S. R.; Hodgson, D. J. *Inorg. Chim. Acta* **1982**, *63*, 141.
(46) Charlot, M. F.; Kahn, O.; Drillon, M. *Chem. Phys.* **1982**, *70*, 177.